RNA m⁶A methyltransferase METTL3 promotes colorectal cancer cell proliferation and invasion by regulating Snail expression

JIANFAN WEN, GUOWEI ZHANG, YUWEN MENG, LEI ZHANG, MIN JIANG and ZHITAO YU

Department of General Surgery, Guangdong Second Provincial General Hospital, Guangzhou, Guangdong 510317, P.R. China

Abstract. Nitrogen 6-methyladenosine (m⁶A) is the result of methylation of nitrogen-6 on adenosine, and is the most abundant chemical modification of eukaryotic mRNA. Dysregulation of m⁶A methylation has been implicated in cancer development and progression through various mechanisms. This type of methylation is primarily regulated by methyltransferase-like 3 (METTL3). However, the molecular mechanisms underlying the role of METTL3 in colorectal cancer (CRC) have not been extensively elucidated. The present study explored m⁶A modification and the underlying mechanism of m⁶A, which serve regulatory roles in the development of CRC. It was found that METTL3 is upregulated in CRC cell lines and tissues, and its expression positively correlated with poor overall survival (OS). Mechanistically, the present study demonstrated that METTL3 methylates Snail mRNA, thus stabilizing it to promote CRC malignancy. The present findings indicate that m⁶A modification is involved in CRC tumorigenesis, and highlight its potential as a therapeutic target against CRC.

Introduction

Colorectal cancer (CRC) is the third most common malignancy worldwide and the main cause of mortality due to tumor metastasis (1). CRC has a high mortality rate when detected at advanced stages. However, the use of stratified treatment options remains limited in standard clinical practice, which indicates that the curative treatment of CRC remains intractable (2). Furthermore, in terms of early diagnosis and successful treatment of CRC (achieving a high overall survival rate), the 5-year survival rate can reach ≤90%, whereas this is reduced to 8% in the case of advanced metastases (3). Previous evidence showed that multistep processes play a role in CRC carcinogenesis, which involves a complicated and dynamic interplay between epigenetics and transcriptomic alterations (4,5). Therefore, it is essential to understand the epigenetic mechanisms underlying CRC to identify promising therapeutic targets.

Previous studies on epigenetics found that nitrogen 6-methyladenosine (m⁶A) RNA modification serves critical roles in the regulation of cell fate, proliferation, metabolism and biogenesis of tumors (6-9). m⁶A modification is the most prevalent modification in eukaryotes, and occurs in mammalian mRNAs (10), long non-coding RNAs (11) and microRNAs (12). It is involved in numerous post-transcriptional functions, including mRNA stability, splicing, transport, localization and translation (13,14). m⁶A methylation is a dynamic epigenetic event primarily modulated by m⁶A writers, erasers and readers (15). Methyltransferase-like 3 (METTL3; M3) was identified as an m⁶A writer that forms a heterodimeric complex with Wilms' tumor 1-associating protein (WTAP) (16) and METTL14 (17) to catalyze m⁶A methylation. By contrast, fat mass and obesity-associated protein (FTO) (18) and α-ketoglutarate-dependent dioxygenase AlkB homolog 5 (ALKBH5) (19) act as m⁶A erasers and participate in m⁶A demethylation. Dysregulation of m⁶A methylation may trigger the progression of various cancer types, including CRC (20). METTL3 has an oncogenic function, and maintains SRY-box transcription factor 2 (SOX2) expression through an m⁶A-insulin like growth factor 2 mRNA binding protein 2 (IGF2BP2)-dependent mechanism in CRC cells (21), which is upregulated in human CRC and promotes CRC progression by enhancing MYC expression (22) and epigenetically suppressing yippee like 5 (23), as well as by stabilizing cyclin E1 mRNA (24). Contrarily, METTL3 was reported as a tumor suppressor in CRC through regulating the p38/ERK signaling pathway (25). These findings reveal that METTL3 acts as a double-edged sword, which affects the progression of CRC via diverse mechanisms and targets. Thus, the role of METTL3 and its specific molecular mechanism in CRC needs to be further explored.

Snail was found to be a critical transcriptional factor for epithelial to mesenchymal transition (EMT), which could promote invasion and proliferation in several cancer types (26). METTL3 can increase mRNA stability and translation efficiency to facilitate proliferation and invasion during

Correspondence to: Professor Zhitao Yu or Professor Jianfan Wen, Department of General Surgery, Guangdong Second Provincial General Hospital, 466 Xingangzhong Street, Guangzhou, Guangdong 510317, P.R. China
E-mail: yuzhitao956@163.com
E-mail: wenjianfan927@163.com

EMT in liver cancer (27), while inhibiting Snail results in the suppression of cell proliferation and motility in CRC (28). However, to the best of our knowledge, the functional link between m^{6}A methylation and Snail in CRC progression has not been established to date.

The present study demonstrated that METTL3 is significantly upregulated in CRC tissues and is associated with poor survival. METTL3 silencing suppresses CRC proliferation and invasion *in vitro*. The present mechanistic studies revealed that METTL3 promotes the expression of Snail via its m^{6}A methylase activity. Gain-and-loss of function experiments revealed that Snail overexpression can counteract the effects of METTL3 knockdown. Overall, the present findings reveal a critical role for the METTL3/Snail axis in CRC progression, thus representing a promising therapeutic strategy for CRC treatment.

Materials and methods

Bioinformatics analysis. Clinical data for bioinformatics analysis were downloaded from the following databases: The Cancer Genome Atlas (TCGA; https://cancergenome.nih.gov/), Gene Expression Profiling Interactive Analysis (GEPIA; https://gepia.cancer-pku.cn/) (29) and Oncomine Platform (www.oncomine.org) (30) analyzed with the R (v3.5.2) and R Bioconductor packages (edgeR; http://bioconductor.org/packages/release/bioc/html/edgeR.html; limma; http://bioconductor.org/packages/release/bioc/html/limma.html).

Patients and tumor samples. Tissue specimens, including five paired CRC tissues and adjacent normal tissues, were obtained from patients with CRC who received treatment at The Guangdong Second Provincial General Hospital (Guangzhou, China) between March and July 2018. The clinical CRC specimens were collected, following ethics approval from the Institutional Research Ethics Committee of The Guangdong Second Provincial General Hospital (approval no. KQ201803 005-GSPGH). All subjects were informed of the investigational nature of the study and provided their written informed consent. Patients were eligible if they were over 18 years of age and had no other concurrent tumors, otherwise they were excluded. Of these patients, three were male (aged 57, 59 and 71 years) and two were female (aged 55 and 63 years). None of the patients had metastatic tumors. Among them, one patient had stage 1 CRC, two patients had stage 2 CRC and the other two patients had stage 3 CRC according to the World Health Organization Classification (31). The tissues were immediately frozen in dry ice and stored at -80°C until further use.

Cell culture, transfection and treatment. The human CRC cell lines HT-29, HCT-116 and SW480; the normal human colon mucosal epithelial cell lines NCM-460 and HIEC-6; and the human cell line 293T were obtained from the Cell Bank of Chinese Academy of Sciences. The HCT-116, SW480 and NCM-460 cell lines were routinely cultured in RPMI-1640 medium with 10% FBS and 1% penicillin-streptomycin in a humidified incubator at 37°C with 5% CO$_2$, while the HT-29 cell line was cultured in McCoy's 5A medium (all from Gibco; Thermo Fisher Scientific, Inc.) under the aforementioned conditions. The HIEC-6 cell line was cultured in complete growth medium, which contained Opti-MEM™ Reduced Serum Medium, 4% FBS, 20 mM HEPES, 10 mM GlutaMAX™ and 10 ng/ml Epidermal Growth Factor (all from Gibco; Thermo Fisher Scientific, Inc.). The 293T cell line was cultured in complete growth medium, which contained Eagle's Minimum Essential Medium (Gibco; Thermo Fisher Scientific, Inc.) and 10% FBS.

A total of 1x10^6 HCT-116 and SW480 cells were seeded into 6-well plates 24 h prior to transfection, and 2,000 ng plasmid (pcDNA3-vector or pcDNA3-Snail; Guangzhou RioboBio Co., Ltd.) per well was transfected into the cells using Lipofectamine® 3000 (Thermo Fisher Scientific, Inc.) according to the manufacturer's instructions.

For the inhibition of METTL3, the HCT-116 and SW480 cells were treated with S-adenosylhomocysteine (100 nM; cat. no. HY-19528; MedChemExpress) for 48 h then the samples were collected and analyzed using western blot analysis.

Establishment of stable knockdown cell lines. A lentivirus-mediated method was used to stably knock down METTL3 expression in HCT-116 and SW480 cells. The sequences used, which were synthesized by Guangzhou RiboBio Co., Ltd., were as follows: Small hairpin (sh) negative control (NC), 5'-TTCTCCGAACGTGTCACGT-3'; shMETTL3-1, 5'-CGTCAGTATCTTGGGCAAGTT-3'; shMETTL3-2, 5'-GCACTTGGATCTACGGAATCC-3'; and shMETTL3-3, 5'-GCAAGTATGTTCACTATGAAA-3'. Lentiviruses were packaged by transfecting the aforementioned shMETTL3 or shNC transfer vector (pLKO.1), psPAX2 and pMD2.G (all from Guangzhou RiboBio Co., Ltd.) under a 3:2:1 ratio into 293T cells. The released virus in the culture medium was collected at 48 and 72 h post-transduction, and was concentrated by ultracentrifugation at 1.7x10^5 x g and 4°C for 2 h.

To construct stable knockdown cells, 1x10^5 HCT-116 and SW480 cells were transduced with shNC or shMETTL3 lentivirus at a multiplicity of infection of 10 with 5 μg/ml polybrene (MilliporeSigma; Merck KGaA) at 37°C for 8 h. The stable expressing cells were screened by treatment with 1 μg/ml puromycin (MilliporeSigma; Merck KGaA) for 1 month.

RNA isolation and reverse transcription-quantitative PCR (RT-qPCR). A total of 5x10^5 HT-29, HCT-116, SW480, NCM-460 and HIEC-6 cells were collected for RNA extraction using TRIzol® (Invitrogen; Thermo Fisher Scientific, Inc.) according to the manufacturer's instructions. Total RNA was reverse transcribed into cDNA using PrimeScript RT Reagent (Takara Bio, Inc.) according to the manufacturer's instructions. Quantification of mRNA expression levels was performed using SYBR® Premix Ex Taq™ Reagent (Takara Bio, Inc.) on a LightCycler® 480 Instrument II (Roche Applied Science). The primers were synthesized by Sangon Biotech Co., Ltd., and their sequences were as follows: METTL3 forward, 5'-CTA TCTCCTGGCACTCGCAAGA-3' and reverse, 5'-GCTTGA ACCGTGCAACCACATC-3'; Snail forward, 5'-TGCCCT CAAGATGCACATCCGA-3' and reverse, 5'-GGGACAGGA GAAGGGCTTCTC-3'; GAPDH forward, 5'-GTCTCCTCT GACTTCAACAGCG-3' and reverse, 5'-ACCACCCTGTTG CTGTAGCCAA-3'; and 18S forward, 5'-CGGACAGGATTG ACAGATTGATAGC-3' and reverse, 5'-GCGTCCTCCTGG

CTGAAGTGG-3'. The expression level was normalized to the mRNA level of GAPDH and was calculated using the $2^{-\Delta\Delta Cq}$ method (32). The following thermocycling conditions were used: Initial denaturation at 95°C for 2 min, followed by 40 cycles at 95°C for 30 sec, 60°C for 25 sec and 72°C for 25 sec.

Protein isolation and western blotting. Total protein from the HCT-116 and SW480 cell lines and tissues was extracted upon lysis with cold RIPA buffer (Beyotime Institute of Biotechnology) containing protease inhibitor cocktail (cat. no. P9599; 1:100; Sigma-Aldrich; Merck KGaA). Total protein concentration was determined by bicinchoninic acid analysis (Beyotime Institute of Biotechnology). The proteins were then separated by 10% SDS-PAGE and transferred onto polyvinylidene difluoride membranes (MilliporeSigma; Merck KGaA). The membranes were blocked with 5% (w/v) skimmed milk at room temperature for 1 h, and incubated with the following primary antibodies: Anti-METTL3 (cat. no. ab195352; Abcam), anti-Snail (cat. no. 3879S, Cell Signaling Technology, Inc.) and anti-GAPDH (cat. no. 5174Ss; Cell Signaling Technology, Inc.) (all at 1,1000) at 4°C overnight, followed by incubation with a horseradish peroxidase (HRP)-conjugate secondary antibody (cat. no. SA00001-1; ProteinTech Group, Inc.; 1:5,000) for 1 h at room temperature. After washing the membranes with 0.01 M TBS containing 0.1% Tween-20 (Sigma-Aldrich; Merck KGaA) three times, the protein bands were visualized with an ECL reagent (Tanon Science and Technology Co., Ltd.) and were detected using a chemiluminescence system (Bio-Rad Laboratories, Inc.). To quantify the change in expression levels of every target, the density of the METTL3 or Snail band in each lane was determined by densitometric analysis using ImageJ software (1.47v; National Institutes of Health), and the relative expression level was normalized to the level of GAPDH.

Immunohistochemistry (IHC). The CRC and adjacent normal tissue were harvested and fixed with 4% paraformaldehyde overnight at 4°C then cut into 5-μm thick sections at -20°C. The tissue slides were then deparaffinized, rehydrated using an alcohol gradient (100, 96 and 70% volume) and subjected to antigen retrieval with sodium citrate buffer. The tissues sections (5-μm) were then blocked with 5% normal goat serum (Vector Laboratories, Inc.; Maravai LifeSciences) with 0.1% Triton X-100 and 3% H_2O_2 in PBS for 60 min at room temperature, and then incubated with an anti-METTL3 antibody (1:200 dilution; cat. no. ab195352; Abcam) at 4°C overnight. IHC staining was performed with a HRP conjugate (1:1,000 dilution; cat. no. SA00001-1; ProteinTech Group, Inc.) using DAB detection. Cell nuclei were counterstained with Hoechst (1:1,000; cat no. 33342; Invitrogen) for 10 min at room temperature. Images were obtained with a Nikon E800 light microscope (magnification, x200; Nikon Corporation) and analyzed with ImageJ software (1.47v; National Institutes of Health). A non-specific antibody (1:200 dilution; cat. no. ab126820; Abcam) was used as a negative control, densitometric analysis of the IHC staining signal of METTL3 was used to analyze any potential significant differences between CRC tissues and adjacent normal tissues by ImageJ software.

Cell proliferation assay. Cell Counting Kit-8 (CCK-8; Dojindo Molecular Technologies, Inc.) assay was used to detect the cellular proliferation of shMETTL3 and shNC cells. The HCT-116 and SW480 cell lines transfected with shM3 and Snail overexpression or NC vector were seeded into a 96-well plate at a density of 5,000 cells per well and cultured at 37°C with 5% CO_2. CCK-8 reagent was added to each well at 0, 24, 48 and 72 h, and then incubated at 37°C for 2 h. Next, the absorbance was read at 450 nm using the PowerWave-X spectrophotometer (BioTek Instruments, Inc.).

Transwell invasion assay. Transwell Matrigel invasion assays were performed using 24-well Transwell inserts with an 8-μm pore size (Corning, Inc.). Briefly, the shNC or shM3 of The HCT-116 and SW480 cell lines transfected with shNC or shM3, or with Snail overexpression vector or NC were seeded into 24-well culture plates pre-coated with Matrigel (BD Biosciences) at 37°C for 4 h for evaluating cell invasion ability. After 24 h, $1x10^5$ cells in 200 μl culture medium without FBS were plated in the upper chambers, while 700 μl culture medium containing 10% FBS was placed in the corresponding bottom chamber and incubated for 24 h at 37°C. The invaded cells were fixed with 4% paraformaldehyde for 15 min and stained with 0.5% crystal violet solution for 30 min at room temperature. Images were randomly obtained from different fields of view, with a Nikon light microscope (magnification, x200; Nikon Corporation). The mean number of invaded cells was calculated by ImageJ software (1.47v; National Institutes of Health) and used to evaluate the invasion capability of the cells.

Wound healing assay. The HCT-116 and SW480 cell lines transfected with shNC or shM3 at a density of $5x10^6$ cells per well were seeded into 6-well plates and grown to 90% confluence in complete medium prior to scratching. Scratches were made in the cell monolayer using a Woundmaker™ tool (Essen Bioscience), and RPMI-1640 medium containing 10% FBS was replaced with medium containing 1% FBS. Images were captured immediately and after wounding at the indicated time points (0, 12, 24 and 48 h), and closure of the wound was monitored using a Nikon light microscope (magnification, x200; Nikon Corporation) and analyzed with ImageJ software (1.47v; National Institutes of Health).

Methylated RNA immunoprecipitation (MeRIP). m^6A qPCR was performed using Magna MeRIP™ m^6A Kit (MilliporeSigma; Merck KGaA) in accordance with the manufacturer's protocol. Briefly, total RNA was extracted from shMETTL3- or shNC-transduced cells with TRIzol® reagent and then treated with DNase R (Qiagen, Inc.). Next, it was randomly fragmented by treatment with chemical reagents, followed by IP with 10 μg anti-m^6A antibody (1:200 dilution; cat. no. ab151230; Abcam) or mouse IgG, which was linked to Magna ChIP™ Protein A+G Magnetic Beads (cat. no. 16-662; MilliporeSigma). After washing with IP buffer [10 mmol/l Tris-HCl, 150 mmol/l NaCl and 0.1% (v/v) IGEPAL® CA-630 (cat. no. I8896; Sigma-Aldrich; Merck KGaA)] three times, the beads were treated with proteinase K (75 μg/ml; cat. no. P2306; Sigma-Aldrich) for 10 min at 55°C with a vortical shaker. Following phenol extraction and ethanol precipitation, the

IgG and m^6A-enriched RNA was reversely transcribed with random hexamers and the enrichment was determined using RT-qPCR (33).

RNA stability assay. To measure the half-life of Snail mRNA, shMETTL3 or shNC cells were seeded at a density of $5x10^6$ cells per well onto 6-wells plates. The CRC and adjacent normal cells were extracted from the tissues using sterile surgical instruments in a biological safety cabinet, then cultured in RPMI-1640 medium supplemented with 10% FBS. These cells were harvested for total RNA isolation and subsequent RT-qPCR analysis as aforementioned at 1, 2, 4 and 8 h after the addition of actinomycin D (Act-D; MilliporeSigma; Merck KGaA) at a final concentration of 5 μg/ml. The regression slope (k) was used to calculate the half-life of Snail mature mRNA according to the equation $t1/2=ln2/k$ (34) and 18S was used for normalization.

Statistical analysis. Data are presented as the mean ± standard deviation. Every experiment was performed independently 3 times. Kaplan-Meier survival curve was analyzed with the log-rank test and the patients were divided into low and high expression level group based on the median expression level (cut-off value, 4.725). Comparisons between CRC and adjacent normal tissues were analyzed with two-tailed paired Student's t-test, whereas data obtained from the cell lines were analyzed by two-tailed unpaired Student's t-test in the case of comparisons between two groups, or by one-way ANOVA followed by Bonferroni correction in the case of multiple comparisons. Statistical analysis was performed with SPSS 19.0 software (IBM Corp.), and graphical representations were conducted with GraphPad Prism version 8.0 software (GraphPad Software, Inc.). $P<0.05$ was considered to indicate a statistically significant difference.

Results

METTL3 is markedly upregulated in CRC and is associated with poor prognosis. To study the effects of m^6A modification on the progression and development of CRC, the expression of m^6A-related enzymes, including METTL3, METTL14 and WTAP, and that of demethyltransferases (FTO and ALKBH5), was evaluated using TCGA database. The results showed that METTL3 expression was significantly upregulated in 222 primary CRC tissues compared with that of 41 normal colonic tissues, while the expression of other enzymes showed negligible differences (Fig. 1A). The GEPIA database, an online tool used for analyzing cancer clinical data originated from TCGA database, showed that METTL3 expression was gradually increased according to clinical stage classification: Clinical stages 1, 2, 3 and 4 (Fig. 1B). Kaplan-Meier curves of OS obtained from the GEPIA database revealed that high expression of METTL3 was associated with less favorable survival (Fig. 1C). Furthermore, increased expression of METTL3 was observed in CRC tissues compared with that in normal tissues using the Oncomine platform (Fig. 1D). Taken together, these bioinformatics outcomes predict that METTL3 is significantly upregulated in CRC and was negatively correlated with clinical stage and OS.

METTL3 expression is markedly increased in CRC. The expression of METTL3 was examined using two human colonic epithelial cell lines (HIEC-6 and NCM-460) and in three CRC cell lines (HT-29, HCT-116 and SW480). RT-qPCR showed that METTL3 was significantly elevated in CRC cell lines compared with its expression in normal epithelial cell lines at the mRNA level (Fig. 2A). The cell lines exhibiting the most significant differences vs. the controls (namely, HCT-116 and SW480) were used in subsequent experiments.

In addition, the mRNA levels of METTL3 were increased in five CRC tissues compared with those in their corresponding adjacent normal tissues according to the results of RT-qPCR (Fig. 2B). Western blotting further confirmed that METTL3 protein expression was significantly increased in five CRC tissues relative to that in normal tissues (Fig. 2C). Furthermore, increased METTL3-positive staining in primary CRC tissues compared with that in normal tissues was detected by IHC (Fig. 2D). Overall, these data indicated that the expression of METTL3 is increased in clinical CRC tissues and cell lines.

METTL3 facilitates the proliferation and migration of CRC in vitro. Based on the results of bioinformatics analysis and the upregulation of METTL3 observed in CRC cell lines and tissues, it was hypothesized that RNA m^6A modification is closely associated with clinicopathological features, and that the m^6A regulator METTL3 may serve an oncogenic role in CRC. Therefore, the effects of METTL3 on the proliferation and migration of CRC cell lines were evaluated.

A scrambled shRNA and three METTL3-silencing shRNAs were constructed, and their knockdown efficiency was evaluated by assessing the mRNA expression level of METTL3 after being transfected into the HCT-116 and SW480 cell lines (Fig. 3A). The results revealed that shM3-3 knockdown was the most efficient shRNA; thus, it was used for constructing the recombinant lentivirus. Upon transduction of the lentivirus in wild-type CRC cell lines, RT-qPCR (Fig. 3B) and western blotting (Fig. 3C) confirmed significant knockdown efficiency of the lentivirus.

Next, stable METTL3 knockdown and corresponding NC of HCT-116 and SW480 cells were generated to analyze the influence on cell proliferation of METTL3 depletion. The results revealed that the proliferation rate of shMETTL3-transduced cells was significantly decreased compared with that of shNC cells (Fig. 3D). In addition, compared with that of shNC cells, shM3 cells exhibited a decreased invasion ability according to the results of Transwell assay (Fig. 3E). Consistently, wound healing assay showed that the downregulation of METTL3 in CRC cell lines suppressed cell migration (Fig. 3F). Collectively, these results indicated that METTL3 promotes the proliferation, migration and invasion of CRC cell lines.

METTL3 promotes the expression of Snail in CRC. In a previous study, Snail exhibited oncogenic roles, and its m^6A modification influenced the progression of liver cancer (24). The present study hypothesized that METTL3 regulates the expression of Snail in a m^6A-dependent manner, thus contributing to CRC malignancy. Initially, the m^6A modification of Snail was assessed in shNC and shM3 cells by MeRIP assay, which identified the presence of m^6A modification in
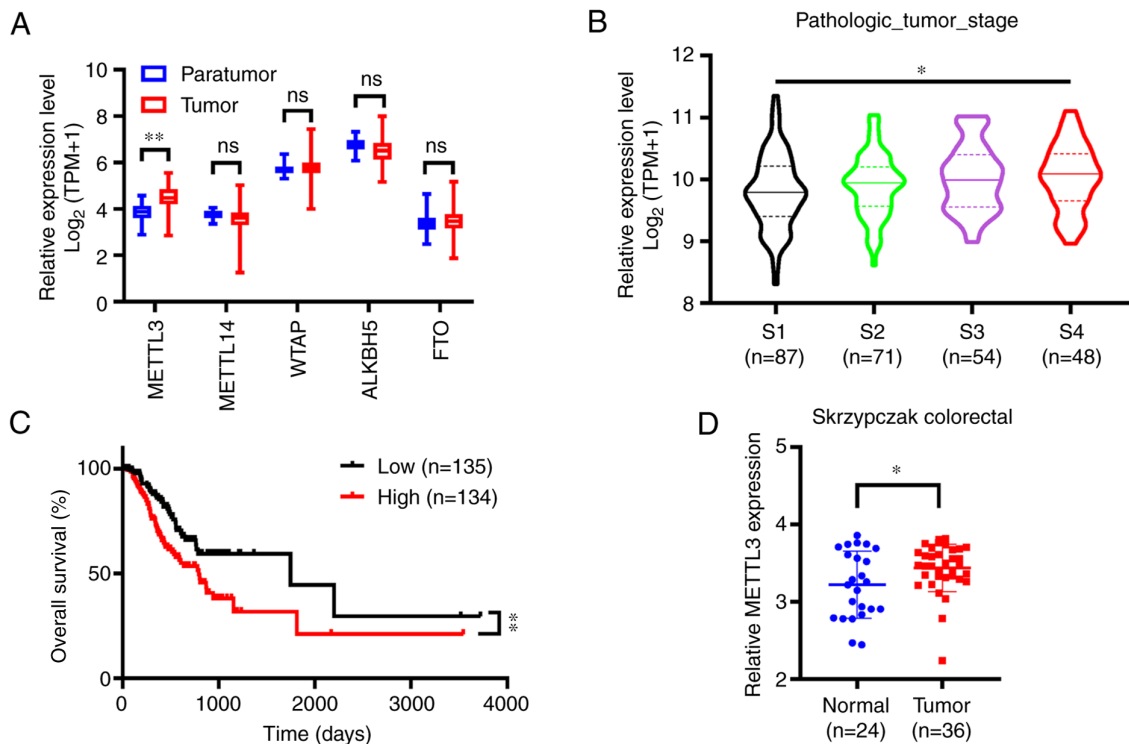
Figure 1. METTL3 is significantly upregulated in CRC on TCGA and Oncomine databases. (A) Nitrogen 6-methyladenosine-related enzymes mRNA expression levels in CRC vs. normal tissues according to TCGA database. (B) METTL3 expression levels in different clinical stages of CRC exhibited the following order: Clinical stages 1, 2, 3 and 4, as represented by the violin plots. (C) The overall survival of patients with CRC who exhibited high (n=135) vs. low (n=134) levels of METTL3 was plotted by the Kaplan-Meier method. (D) METTL3 mRNA expression levels in CRC and normal tissues according to the Oncomine database 'Skrzypczak colorectal'. Error bars represent standard deviation. $^*P<0.05$, $^{**}P<0.01$. METTL3, methyltransferase-like 3; CRC, colorectal cancer; TCGA, The Cancer Genome Atlas; TPM, transcript count per million; ns, not significant; WTAP, Wilms' tumor 1-associating protein; ALKBH5, α-ketoglutarate-dependent dioxygenase AlkB homolog 5; FTO, fat mass and obesity-associated protein.

shNC HCT-116 cells, while this enrichment was significantly decreased in shM3 HCT-116 cells (Fig. 4A). Consistently, m^6A enrichment was increased in shNC SW480 cells compared with that in shMETTL3-infected SW480 cells (Fig. 4B).

Furthermore, western blotting revealed that the expression of Snail was elevated in shNC cells compared with that in shM3 cells (Fig. 4C). The mRNA expression level of Snail was also evaluated in shNC- and shMETTL3-infected cells, and, similarly, it was observed that the mRNA level of Snail in shMETTL3-infected cells was downregulated (Fig. 4D). Inhibiting METTL3 could decrease Snail expression by addition of an METTL3 inhibitor, akin to METTL3 knockout (Fig. 4E). To investigate the potential mechanism responsible for the downregulation of Snail in shM3 cells, the decay rate of Snail mRNA in shNC and shM3 cells was determined by adding Act-D at the indicated time points, and the results showed that the mRNA stability of Snail was significantly reduced in shMETTL3-infected cells (Fig. 4F). As expected, the mRNA stability of Snail in CRC tissues was higher than that in colon normal tissues (Fig. 4G).

These findings demonstrate that Snail is a direct downstream effector of METTL3-induced malignancy. To characterize the potential role of Snail in CRC malignancy, gain- and loss-of-function experiments were performed by overexpressing Snail in shM3 and shNC cells. It was observed that Snail overexpression promoted the proliferation rate of HCT-116 cells and reversed the effects of METTL3 knockdown in HCT-116 cells (Fig. 4H). Consistently, overexpression of Snail alleviates the shMETTL3-induced proliferation suppression in SW480 cells (Fig. 4I). Furthermore, Snail overexpression rescued the invasive potential of METTL3-silenced HCT-116 cells (Fig. 4J). Taken together, these results indicate that METTL3 promotes the growth and invasion of CRC through regulating the level of Snail mRNA *in vitro*.

Discussion

Recently, m^6A modification has gained attention in the field of epigenomics (35). Previous studies have indicated that m^6A regulators serve important regulatory roles in diverse biological processes in various human cancer types, including breast and lung cancer and CRC (36-38). METTL3, as the most important writer of m^6A, is upregulated in numerous malignancies and can epigenetically increase gene expression by specifically editing m^6A sites modification, thus eliciting a potential malignant function (39). Previous studies have demonstrated that METTL3 is frequently upregulated in CRC, where it maintains high m^6A modification levels (40-42). Consistently, the present data showed that METTL3 is elevated in five paired CRC tissues and CRC cell lines. Together with the previously published results in the literature, the present findings supported that m^6A and elevated METTL3 may participate in CRC progression. However, the number of clinical samples is too small in the present study; therefore, additional paired clinical CRC tissues are required to further support the conclusions in future studies.
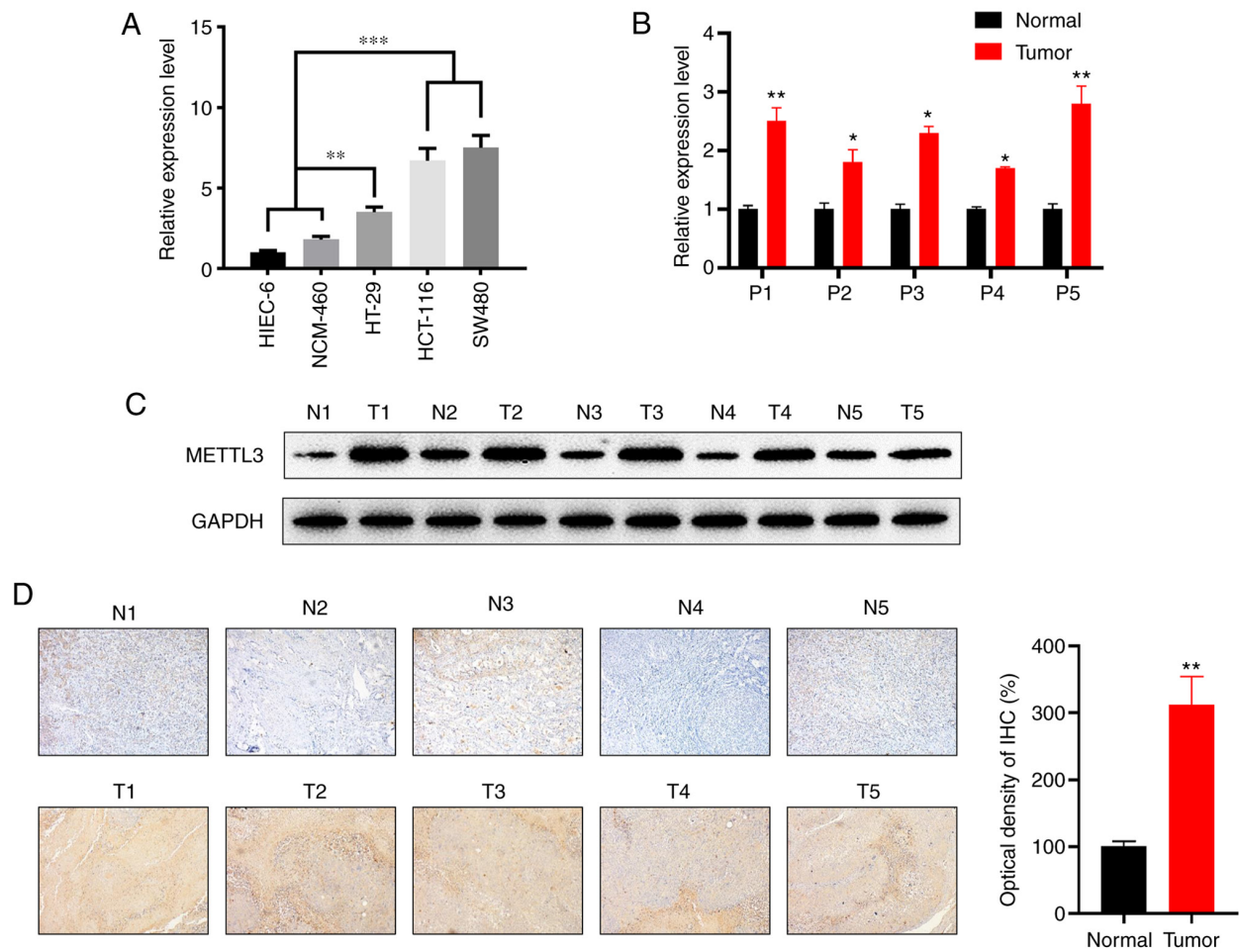
Figure 2. METTL3 is significantly upregulated in CRC tissues compared with its expression levels in the corresponding adjacent normal colon tissues. (A) METTL3 mRNA expression levels in the human CRC cell lines, HT-29, HCT-116 and SW480, the normal cell lines NCM-460 and HIEC-6. (B) Relative mRNA expression levels of METTL3 in CRC tissues compared with those in the corresponding adjacent normal tissues (n=5). (C) Protein expression of METTL3 in CRC vs. the corresponding adjacent normal tissues. GAPDH was used as a loading control. The right panel shows the quantitative analysis of the western blot results, as analyzed by paired Student's t-test. (D) The expression of METTL3 in CRC and adjacent normal tissues was detected by IHC staining (magnification, x100; n=5). Error bars represent standard deviation. *P<0.05, **P<0.01, ***P<0.001. METTL3, methyltransferase-like 3; CRC, colorectal cancer; P, patient; N, normal; T, tumor.

The present study evaluated the effects of METTL3 in CRC using lentivirus-mediated METTL3 knockdown assays, and the results showed that the suppression of METTL3 decreased the invasion, migration and proliferation of the CRC cell lines *in vitro*. A previous study demonstrated that METTL3 silencing in CRC patient-derived organoids and transgenic mouse models exhibited anticancer effects by inhibiting the translation of glucose transporter 1 *in vivo* (43). Furthermore, knockdown of METTL3 suppressed cell proliferation and migration in SW620 and HT29 cells (23). These findings indicate that METTL3 serves oncogenic and pivotal roles in CRC carcinogenesis *in vitro* and *in vivo*, which suggests that targeting METTL3 and developing m⁶A inhibitors may be a novel approach for CRC therapy.

m⁶A modification is a complex regulatory network that participates in various stages of the RNA life cycle and metabolism, including RNA processing, nuclear output, regulation of translation and RNA degradation (44). Using m⁶A-RIP-qPCR and Act-D assays, the present study demonstrated that METTL3-mediated m⁶A enrichment enhances the stability of Snail mRNA during RNA processing. However, other post-transcriptional processes were not evaluated and remain to be investigated further. m⁶A reader proteins, including IGF2BP1/2/3, eukaryotic initiation factor 3 and YTH domain family, members 1/2/3, can bind to an m⁶A-modified motif indirectly or directly, thus affecting RNA function (45). A previous study reported that IGF2BP2 can recognize methylated SOX2 transcripts in the coding sequence regions to prevent SOX2 mRNA degradation, which contributes to the malignant behavior of CRC (21). The present findings demonstrate that m⁶A can stabilize Snail mature mRNA. However, further studies are required to characterize the Snail mRNA m⁶A editing sites and m⁶A readers are involved in their mRNA degradation.

Snail activates EMT signals and pathways as a transcriptional factor, which can affect cancer progression and the metastatic potential of tumors (46). The present study confirmed that overexpression of Snail could increase the proliferation and migration of the CRC cell lines. Phosphorylation and ubiquitination of Snail induce protein degradation, which can reverse tumorigenesis (47). The present study has showed that METTL3 depletion can repress
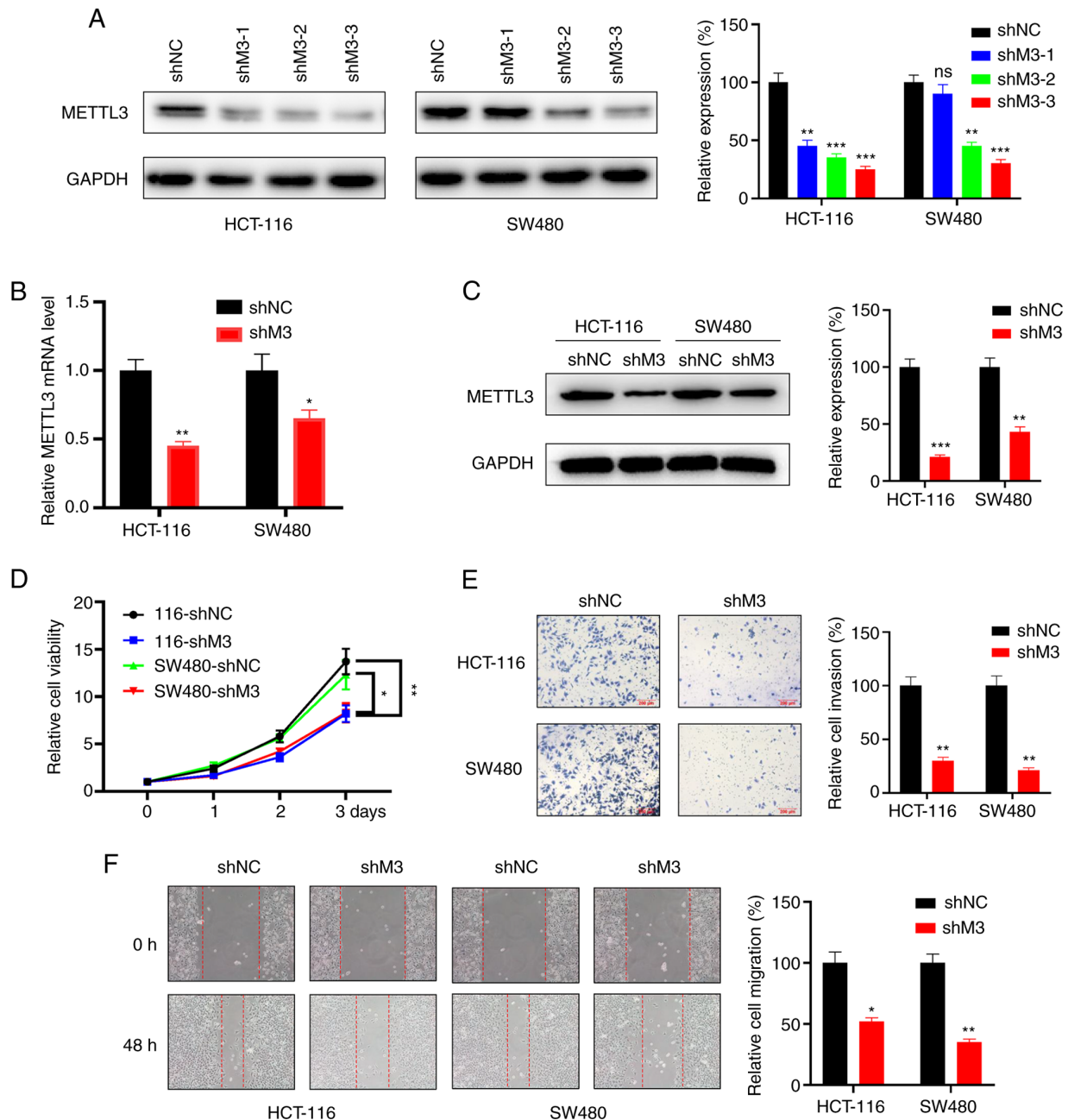
Figure 3. M3 knockdown represses cell proliferation, invasion and migration *in vitro*. (A) Protein levels (right, quantitative analysis) of M3 in HCT-116 and SW480 cells upon transfection with a scrambled shRNA or with one of three different M3-silencing shRNAs. (B) mRNA levels of M3 in HCT-116 and SW480 cells infected with lentivirus carrying the indicated shRNA. (C) Protein levels of M3 in HCT-116 and SW480 cells infected with lentivirus carrying the indicated shRNA (right, quantitative analysis). (D) The proliferation rate of stable scrambled shRNA (shNC) and stable METTL3 knockdown (shM3) cells was evaluated by Cell Counting Kit-8 assay in HCT-116 and SW480 cells. (E) Transwell assay (right, quantitative analysis) was employed to analyze the difference in the invasion ability of shNC and shM3 cells. (F) Wound healing assay (magnification, x200; right, quantitative analysis) revealed differences in the migration ability of shNC and shM3 cells. Each experiment was repeated three times independently. Error bars represent standard deviation. *$P<0.05$, **$P<0.01$, ***$P<0.001$. M3, methyltransferase-like 3; sh, small hairpin RNA; NC, negative control; ns, not significant.

Snail in an m^6A-dependent manner at the RNA level, indicating that targeting Snail mRNA m^6A sites to induce the suppression of expression may be a novel method to prevent CRC progression.

The present study used bioinformatics analysis to screen potential targets, including Snail and METTL3, which were confirmed in clinical tissues, and explored the mechanisms and functions of the targets involved in CRC progression. The present findings provide novel information on the participation of the m^6A epitranscriptome in cancer progression.

In summary, the present study confirmed that METTL3 acts as a critical m^6A methyltransferase capable of facilitating CRC progression, and revealed a novel mechanism by which METTL3 promotes CRC cell proliferation and invasion via stabilizing Snail mRNA in an m^6A-dependent manner. Additionally, the present results indicated that the upregulation of METTL3 may be a major driver of CRC progression *in vitro* and *in vivo*. Overall, these results suggest that targeting METTL3 and Snail may represent promising therapeutic strategies for the treatment of CRC.
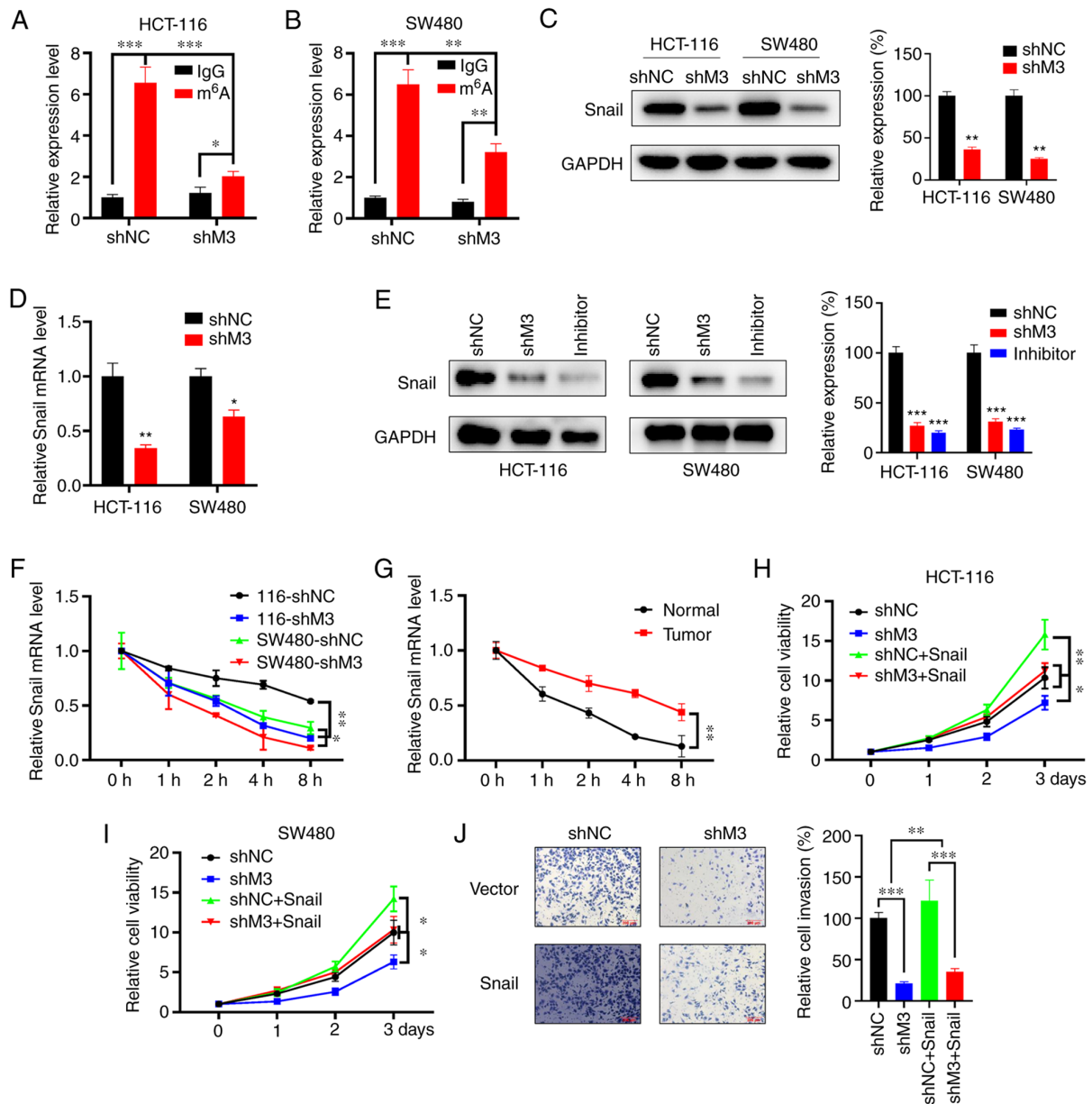
Figure 4. Snail mediates M3-induced malignancy in CRC. m⁶A RIP-qPCR analysis of Snai1 mRNA in shNC- and shM3-infected (A) HCT-116 and (B) SW480 cells. (C) Snail protein expression levels (right, quantitative analysis) in stable with/without M3 knockdown HCT-116 and SW480 cells. (D) Snail mRNA expression levels in stably infected HCT-116 and SW480 cells with/without M3 knockdown. (E) Wild-type cells were treated with S-adenosylhomocysteine at a final concentration of 100 nM for 48 h, followed by detection of Snail protein expression (right, quantitative analysis) using western blot analysis. shNC and shM3 cells were included for analysis. (F) Snail mRNA expression levels in shNC and shM3 cells treated with Act-D (5 μg/ml) for the indicated time points were evaluated by qPCR. (G) Snail mRNA expression levels in CRC and adjacent normal tissue cells treated with Act-D (5 μg/ml) for the indicated time points were evaluated by qPCR. The proliferation rate of (H) HCT-116 and (I) SW480 cells transfected with shNC and shM3 and/or overexpressing Snail was evaluated using a Cell Counting Kit-8 assay at the indicated time points. (J) shNC or shM3 cells transiently overexpressing Snail or pcDNA3 vector were subjected to invasion assays for 24 h and subsequently analyzed with CytoSelect™ 24-well Cell Invasion assay kits (magnification, x100; 8 μm; left). The invaded cells were then quantitatively analyzed (right). All experiments were performed in triplicate. Error bars represent standard deviation. *P<0.05, **P<0.01, ***P<0.001. M3, methyltransferase-like 3; CRC, colorectal cancer; m⁶A, nitrogen 6-methyladenosine; RIP, RNA immunoprecipitation; qPCR, quantitative PCR; sh, small hairpin RNA; NC, negative control; Act-D, actinomycin D.

Availability of data and materials

All data generated and/or analyzed during this study are included in this published article.

Authors' contributions

Conception and design: JW, GZ and ZY; acquisition of data: JW, YM and LZ; statistical analysis: JW, GZ and MJ; writing

and revision of the manuscript: JW and ZY. JW and ZY confirmed the authenticity of all the raw data. All authors read and approved the final manuscript.

Ethics approval and consent to participate

All the study procedures involving human participants were conducted in accordance with the ethical standards of the institutional research committee (approval no. KQ201803005-GSPGH) and patients provided written informed consent.

Patient consent for publication

Not applicable.

Competing interests

The authors declare that they have no competing interests.

References

1. Siegel RL, Miller KD, Fedewa SA, Ahnen DJ, Meester RG, Barzi A and Jemal A: Colorectal cancer statistics, 2017. CA Cancer J Clin 67: 177-193, 2017.
2. National Health Commission of The People's Republic of China: National guidelines for diagnosis and treatment of colorectal cancer 2020 in China (English version). Chin J Cancer Res 32: 415-445, 2020.
3. Degiuli M, Reddavid R, Ricceri F, Di Candido F, Ortenzi M, Elmore U, Belluco C, Rosati R, Guerrieri M and Spinelli A; Members of the Italian Society of Surgical Oncology Colorectal Cancer Network (SICO-CCN) Collaborative Group: Segmental colonic resection is a safe and effective treatment option for colon cancer of the splenic flexure: A nationwide retrospective study of the italian society of surgical oncology-colorectal cancer network collaborative group. Dis Colon Rectum 63: 1372-1382, 2020.
4. Tang R, Cheng AJ, Wang JY and Wang TC: Close correlation between telomerase expression and adenomatous polyp progression in multistep colorectal carcinogenesis. Cancer Res 58: 4052-4054, 1998.
5. Pichler M, Stiegelbauer V, Vychytilova-Faltejskova P, Ivan C, Ling H, Winter E, Zhang X, Goblirsch M, Wulf-Goldenberg A, Ohtsuka M, et al: Genome-Wide miRNA analysis identifies miR-188-3p as a novel prognostic marker and molecular factor involved in colorectal carcinogenesis. Clin Cancer Res 23: 1323-1333, 2017.
6. Sun T, Wu R and Ming L: The role of m6A RNA methylation in cancer. Biomed Pharmacother 112: 108613, 2019.
7. Zhang C, Chen Y, Sun B, Wang L, Yang Y, Ma D, Lv J, Heng J, Ding Y, Xue Y, et al: m6A modulates haematopoietic stem and progenitor cell specification. Nature 549: 273-276, 2017.
8. Di Timoteo G, Dattilo D, Centron-Broco A, Colantoni A, Guarnacci M, Rossi F, Incarnato D, Oliviero S, Fatica A, Morlando M and Bozzoni I: Modulation of circRNA metabolism by m6A modification. Cell Rep 31: 107641, 2020.
9. Chen F, Chen Z, Guan T, Zhou Y, Ge L, Zhang H, Wu Y, Jiang GM, He W, Li J and Wang H: N6-Methyladenosine regulates mRNA stability and translation efficiency of KRT7 to promote breast cancer lung metastasis. Cancer Res 81: 2847-2860, 2021.
10. Meyer KD, Saletore Y, Zumbo P, Elemento O, Mason CE and Jaffrey SR: Comprehensive analysis of mRNA methylation reveals enrichment in 3'UTRs and near stop codons. Cell 149: 1635-1646, 2012.
11. Wu Y, Yang X, Chen Z, Tian L, Jiang G, Chen F, Li J, An P, Lu L, Luo N, et al: m6A-induced lncRNA RP11 triggers the dissemination of colorectal cancer cells via upregulation of Zeb1. Mol Cancer 18: 87, 2019.
12. Alarcon CR, Lee H, Goodarzi H, Halberg N and Tavazoie SF: N6-methyladenosine marks primary microRNAs for processing. Nature 519: 482-485, 2015.
13. Wang X, Lu Z, Gomez A, Hon GC, Yue Y, Han D, Fu Y, Parisien M, Dai Q, Jia G, et al: N6-methyladenosine-dependent regulation of messenger RNA stability. Nature 505: 117-120, 2014.
14. Wang X, Zhao BS, Roundtree IA, Lu Z, Han D, Ma H, Weng X, Chen K, Shi H and He C: N6-methyladenosine modulates messenger RNA translation efficiency. Cell 161: 1388-1399, 2015.
15. Jia G, Fu Y and He C: Reversible RNA adenosine methylation in biological regulation. Trends Genet 29: 108-115, 2013.
16. Schwartz S, Mumbach MR, Jovanovic M, Wang T, Maciag K, Bushkin GG, Mertins P, Ter-Ovanesyan D, Habib N, Cacchiarelli D, et al: Perturbation of m6A writers reveals two distinct classes of mRNA methylation at internal and 5'sites. Cell Rep 8: 284-296, 2014.
17. Zhou T, Ren Z and Chen C: METTL14 as a predictor of postoperative survival outcomes of patients with hepatocellular carcinoma. Nan Fang Yi Ke Da Xue Xue Bao 40: 567-572, 2020 (In Chinese).
18. Mathiyalagan P, Adamiak M, Mayourian J, Sassi Y, Liang Y, Agarwal N, Jha D, Zhang S, Kohlbrenner E, Chepurko E, et al: FTO-Dependent N6-methyladenosine regulates cardiac function during remodeling and repair. Circulation 139: 518-532, 2019.
19. Xu K, Mo Y, Li D, Yu Q, Wang L, Lin F, Kong C, Balelang MF, Zhang A, Chen S, et al: N6-methyladenosine demethylases Alkbh5/Fto regulate cerebral ischemia-reperfusion injury. Ther Adv Chronic Dis 11: 2040622320916024, 2020.
20. Zhang J, Cheng X, Wang J, Huang Y, Yuan J and Guo D: Gene signature and prognostic merit of M6a regulators in colorectal cancer. Exp Biol Med (Maywood) 245: 1344-1354, 2020.
21. Li T, Hu PS, Zuo Z, Lin JF, Li X, Wu QN, Chen ZH, Zeng ZL, Wang F, Zheng J, et al: METTL3 facilitates tumor progression via an m6A-IGF2BP2-dependent mechanism in colorectal carcinoma. Mol Cancer 18: 112, 2019.
22. Yang DD, Chen ZH, Yu K, Lu JH, Wu QN, Wang Y, Ju HQ, Xu RH, Liu ZX and Zeng ZL: METTL3 Promotes the progression of gastric cancer via targeting the MYC Pathway. Front Oncol 10: 115, 2020.
23. Zhou D, Tang W, Xu Y, Xu Y, Xu B, Fu S, Wang Y, Chen F, Chen Y, Han Y and Wang G: METTL3/YTHDF2 m6A axis accelerates colorectal carcinogenesis through epigenetically suppressing YPEL5. Mol Oncol: Jan 7, 2021 doi: 10.1002/1878-0261.12898 (Epub ahead of print).
24. Zhu W, Si Y, Xu J, Lin Y, Wang JZ, Cao M, Sun S, Ding Q, Zhu L and Wei JF: Methyltransferase like 3 promotes colorectal cancer proliferation by stabilizing CCNE1 mRNA in an m6A-dependent manner. J Cell Mol Med 24: 3521-3533, 2020.
25. Deng R, Cheng Y, Ye S, Zhang J, Huang R, Li P, Liu H, Deng Q, Wu X, Lan P and Deng Y: m6A methyltransferase METTL3 suppresses colorectal cancer proliferation and migration through p38/ERK pathways. Onco Targets Ther 12: 4391-4402, 2019.
26. Yu X, Zhao H and Cao Z: The m6A methyltransferase METTL3 aggravates the progression of nasopharyngeal carcinoma through inducing EMT by m6A-modified Snail mRNA. Minerva Med: Jun 5, 2020 doi: 10.23736/S0026-4806.20.06653-7 (Epub ahead of print).
27. Lin X, Chai G, Wu Y, Li J, Chen F, Liu J, Luo G, Tauler J, Du J, Lin S, et al: RNA m(6)A methylation regulates the epithelial mesenchymal transition of cancer cells and translation of Snail. Nat Commun 10: 2065, 2019.
28. Wang Y, Wu Z and Hu L: The regulatory effects of metformin on the [SNAIL/miR-34]:[ZEB/miR-200] system in the epithelial-mesenchymal transition(EMT) for colorectal cancer(CRC). Eur J Pharmacol 834: 45-53, 2018.
29. Tang Z, Li C, Kang B, Gao G, Li C and Zhang Z: GEPIA: A web server for cancer and normal gene expression profiling and interactive analyses. Nucleic Acids Res 45: W98-W102, 2017.
30. Rhodes DR, Yu J, Shanker K, Deshpande N, Varambally R, Ghosh D, Barrette T, Pandey A and Chinnaiyan AM: ONCOMINE: A cancer microarray database and integrated data-mining platform. Neoplasia 6: 1-6, 2004.
31. Ahadi M, Sokolova A, Brown I, Chou A and Gill AJ: The 2019 World Health Organization Classification of appendiceal, colorectal and anal canal tumours: An update and critical assessment. Pathology 53: 454-461, 2021.
32. Livak KJ and Schmittgen TD: Analysis of relative gene expression data using real-time quantitative PCR and the 2(-Delta Delta C(T)) method. Methods 25: 402-408, 2001.
33. Dominissini D, Moshitch-Moshkovitz S, Schwartz S, Salmon-Divon M, Ungar L, Osenberg S, Cesarkas K, Jacob-Hirsch J, Amariglio N, Kupiec M, et al: Topology of the human and mouse m6A RNA methylomes revealed by m6A-seq. Nature 485: 201-206, 2012.
34. Hentze MW: Determinants and regulation of cytoplasmic mRNA stability in eukaryotic cells. Biochim Biophys Acta 1090: 281-292, 1991.

35. Yang G, Sun Z and Zhang N: Reshaping the role of m⁶A modification in cancer transcriptome: A review. Cancer Cell Int 20: 353, 2020.
36. Wu L, Wu D, Ning J, Liu W and Zhang D: Changes of N⁶-methyladenosine modulators promote breast cancer progression. BMC Cancer 19: 326, 2019.
37. Wang H, Zhao X and Lu Z: m⁶A RNA methylation regulators act as potential prognostic biomarkers in lung adenocarcinoma. Front Genet 12: 622233, 2021.
38. Tian J, Ying P, Ke J, Zhu Y, Yang Y, Gong Y, Zou D, Peng X, Yang N, Wang X, *et al*: ANKLE1 N⁶-Methyladenosine-related variant is associated with colorectal cancer risk by maintaining the genomic stability. Int J Cancer 146: 3281-3293, 2020.
39. Huo FC, Zhu ZM, Zhu WT, Du QY, Liang J and Mou J: METTL3-mediated m⁶A methylation of SPHK2 promotes gastric cancer progression by targeting KLF2. Oncogene 40: 2968-2981, 2021.
40. Lan H, Liu Y, Liu J, Wang X, Guan Z, Du J and Jin K: Tumor-associated macrophages promote oxaliplatin resistance via METTL3-mediated m⁶A of TRAF5 and necroptosis in colorectal cancer. Mol Pharm 18: 1026-1037, 2021.
41. Chen H, Gao S, Liu W, Wong CC, Wu J, Wu J, Liu D, Gou H, Kang W, Zhai J, *et al*: RNA N⁶-Methyladenosine methyltransferase METTL3 facilitates colorectal cancer by activating the m⁶A-GLUT1-mTORC1 axis and is a therapeutic target. Gastroenterology 160: 1284-1300.e16, 2021.
42. Peng W, Li J, Chen R, Gu Q, Yang P, Qian W, Ji D, Wang Q, Zhang Z, Tang J and Sun Y: Upregulated METTL3 promotes metastasis of colorectal Cancer via miR-1246/SPRED2/MAPK signaling pathway. J Exp Clin Cancer Res 38: 393, 2019.
43. Shen C, Xuan B, Yan T, Ma Y, Xu P, Tian X, Zhang X, Cao Y, Ma D, Zhu X, *et al*: m⁶A-dependent glycolysis enhances colorectal cancer progression. Mol Cancer 19: 72, 2020.
44. Yang Y, Hsu PJ, Chen YS and Yang YG: Dynamic transcriptomic m⁶A decoration: Writers, erasers, readers and functions in RNA metabolism. Cell Res 28: 616-624, 2018.
45. Zhen D, Wu Y, Zhang Y, Chen K, Song B, Xu H, Tang Y, Wei Z and Meng J: m⁶A Reader: Epitranscriptome target prediction and functional characterization of N⁶-methyladenosine (m⁶A) readers. Front Cell Dev Biol 8: 741, 2020.
46. Kudo-Saito C, Shirako H, Takeuchi T and Kawakami Y: Cancer metastasis is accelerated through immunosuppression during Snail-induced EMT of cancer cells. Cancer Cell 15: 195-206, 2009.
47. Dominguez D, Montserrat-Sentís B, Virgós-Soler A, Guaita S, Grueso J, Porta M, Puig I, Baulida J, Francí C and García de Herreros A: Phosphorylation regulates the subcellular location and activity of the snail transcriptional repressor. Mol Cell Biol 23: 5078-5089, 2003.